0026-895X/02/6102-425–435$3.00
MOLECULAR PHARMACOLOGY
Copyright © 2002 The American Society for Pharmacology and Experimental Therapeutics
Mol Pharmacol 61:425–435, 2002

Vol. 61, No. 2
1109/961624
Printed in U.S.A.

The Thiol Sensitivity of Glutathione Transport in Sidedness-Sorted Basolateral Liver Plasma Membrane and in Oatp1-Expressing HeLa Cell Membrane

ARAVIND MITTUR, ALLAN W. WOLKOFF, and NEIL KAPLOWITZ

Research Center for Liver Diseases, Department of Medicine, University of Southern California, Los Angeles, California (A.M., N.K.); and Marion Bessin Liver Research Center, Albert Einstein College of Medicine, Bronx, New York (A.W.W.)

Received May 15 2001; accepted November 13, 2001

This paper is available online at http://molpharm.aspetjournals.org

ABSTRACT

Sinusoidal efflux of hepatic reduced glutathione (GSH) is a key step in interorgan GSH/cysteine homeostasis and extracellular detoxification. Rat organic anion transporter polypeptide1 (Oatp1) is known to transport GSH but several features of sinusoidal GSH uptake, such as electrogenic property and asymmetric effects of uncharged thiols (increased efflux, decreased uptake), either cannot be accounted for by Oatp1 or have not been studied. The asymmetric effect of thiols has only been studied in intact cells and not directly in membrane vesicles. To accomplish the latter, we studied GSH uptake in inside-out–(IO) and rightside-out–(RO) oriented basolateral plasma membrane vesicles (bLPM). We also studied the kinetics and effect of thiols on GSH transport by Oatp1 stably expressed in HeLa cells. GSH uptake was ~2- to 3-fold higher in IO than RO bLPM. Dithiothreitol-stimulated GSH uptake in IO but inhibited uptake in RO bLPM, demonstrating that thiols exert direct asymmetric side-specific effects on GSH transport. Uptake in IO and RO bLPM was sigmoid (K_m ~13 mM) with a 2-fold higher capacity in IO compared with RO bLPM. In both IO and RO bLPM, a component with a high affinity but low capacity for GSH (K_m ~100 μM) was also present. Endogenous GSH transporter in HeLa cells was thiol-sensitive, electrogenic, and described by a single Michaelis-Menten component (K_m ~15 mM). In contrast, GSH transport mediated by Oatp1 was insensitive to thiols and membrane potential, inhibited by cystine, and stimulated by an inward H^+ gradient. These findings identify novel functional asymmetries in sinusoidal efflux and uptake of GSH and further clarify the role of Oatp1 in GSH transport.

The cellular level of GSH is maintained by at least four processes: efflux and uptake of intact GSH; uptake of precursors by amino acid transporters; intracellular synthesis; and utilization. Transport may be the predominant process for maintaining intracellular pools of GSH when synthesis of GSH is minimal. Transport of GSH from hepatocytes is bidirectional and GSH is exported into blood and bile by transporters in the sinusoidal and canalicular plasma membrane domains, respectively (Kaplowitz et al., 1985, 1990; Garcia-Ruiz et al., 1992; Ookhtens and Kaplowitz, 1998). Sinusoidal efflux is critical in interorgan homeostasis of GSH and thiol-disulfides (Ookhtens and Kaplowitz, 1998) and presumably in regulation of redox status in plasma. Carrier-mediated transport of GSH across the sinusoidal membrane of hepatocytes is mediated by high- and low-affinity components (Inoue et al., 1984; Ookhtens et al., 1985; Aw et al., 1986; Mittur et al., 2000). GSH transport in perfused livers, hepatocytes, and basolateral plasma membrane vesicles (bLPM) is mediated by a low-affinity transporter with sigmoid kinetics (K_m ~3–12 mM; n_H ~2–3). The role of the high-affinity component (K_m ~150 μM) in regulation of sinusoidal GSH efflux is not clear because it has a 10-fold lower capacity than the low-affinity component and is saturated at normal cellular levels of GSH (Aw et al., 1986; Mittur et al., 2000). A functional size of ~70 kDa has been estimated for the high-affinity component observed in bLPM (Mittur et al., 2000).

Sinusoidal GSH efflux is *trans*-inhibited by methionine and cystathionine (Aw et al., 1986; Ghibelli et al., 1998), *cis*-inhibited by unconjugated and mono- and diglucuronide forms of bilirubin, and sulfobromophthalein-glutathione conjugate (Aw et al., 1986; Ookhtens et al., 1988; Fernandez-Checa et al., 1993). Certain disulfides (cystine and oxidized glutathione disulfide) and uncharged thiols such as dithiothreitol (DTT) have opposite effects on low-affinity, high-

This study was supported by National Institutes of Health grants DK30312 (N.K.) and DK23026 (A.W.). The Kinetic and Mathematical Modeling Core of USC Research Center for Liver Diseases was supported in part by grant P30-DK48522.

ABBREVIATIONS: GSH, reduced glutathione; bLPM, basolateral plasma membrane vesicles; n_H, number of binding/transport sites for a substrate in transport system; DTT, dithiothreitol; IO, inside-out; RO, rightside-out; Oatp1, rat organic anion transporter polypeptide1; Oatp2, rat organic anion transporter polypeptide2; cLPM, canalicular plasma membrane vesicles.

capacity sinusoidal GSH transport (Lu et al., 1993, 1994). Disulfides decrease maximal efflux of GSH from cultured hepatocytes and perfused liver but uncharged thiols enhance efflux by up to 400% (Lu et al., 1993, 1994). Conversely, DTT inhibits GSH uptake in cultured hepatocytes. Observations on the influence of thiols and disulfides on GSH transport in hepatocytes and perfused livers cannot differentiate their mechanisms of action from multiple possibilities, such as direct effects on transporter(s) and/or intracellular actions. Thus, the specific mechanisms and sites of action of thiols and disulfides on sinusoidal GSH transport are unknown. Examining transport in membrane vesicles can establish whether thiols and disulfides influence GSH transport at the level of transporters. However, membrane vesicles used in the past were a mixed population of inside-out (IO) and rightside-out (RO) orientated vesicles and thus unable to differentiate the side-specific effects of thiols on efflux and uptake of GSH.

Expression of the Na^+-independent rat organic anion transporter polypeptide 1 (Oatp1) in *Xenopus laevis* oocytes enhances the efflux of GSH in exchange with taurocholate (Li et al., 1998). However, DTT, methionine, and cystathionine do not influence transport of taurocholate by Oatp1 (Li et al., 1998). On the other hand, effects of thiols on Oatp1-mediated GSH transport are not known. The transport of substrates by Oatp1 is expected to be an electroneutral process, whereas high-capacity transport of GSH with sinusoidal characteristics is electrogenic (Aw et al., 1984; Fernandez-Checa et al., 1993). Partly because of these discrepancies, the contribution of Oatp1 to hepatic sinusoidal GSH transport is not clear. The kinetic characteristics of GSH transport mediated by Oatp1 are also unknown and need to be correlated with hepatic sinusoidal transport. Other transporters, including a thiol-sensitive carrier, may exist as major transporter(s) of hepatic sinusoidal GSH. GSH is a poor substrate for the rat organic anion transporter polypeptide 2 (Oatp2) but an optimal level of intracellular GSH is necessary for uptake of taurocholate and digoxin by Oatp2 (Li et al., 2000). GSH does not seem to exchange with these substrates (Li et al., 2000).

We examined GSH uptake in well-separated IO and RO bLPM to answer the following: 1) Do thiols exert their effect on GSH uptake at the level of plasma membrane; if so, are their effects on uptake in sidedness-sorted bLPM different, and 2) Are rates of GSH efflux and uptake different? In addition, we examined the role of Oatp1 in total sinusoidal GSH transport by characterizing GSH transport in HeLa cells that over-express Oatp1 by: 1) identifying and comparing kinetics of GSH transport in membrane vesicles from HeLa cells expressing Oatp1 to side-sorted hepatic sinusoidal transport, and 2) testing the sensitivity of GSH transport mediated by Oatp1 to thiols and disulfides.

Materials and Methods

Chemicals. All chemicals and reagents were purchased from Sigma Chemical Co. (St. Louis, MO) or other reputable commercial sources. Concanavalin A-Sepharose 4B was purchased from Amersham Biosciences (Piscataway, NJ) and washed free of ethanol before use. [^{35}S]GSH (>100 Ci/mmol), [^{3}H]alanine (>75 Ci/mmol), [^{3}H]taurocholic acid (>2 Ci/mmol), [^{3}H]*l*-glutamate (>40 Ci/mmol), [^{3}H]leukotriene C4 (>110 Ci/mmol), and Aquasol scintillation cocktail were procured from PerkinElmer Life Sciences (Boston, MA). The purity and chemical form of [^{35}S]GSH was confirmed by radioactive high-performance liquid chromatography (Fariss and Reed, 1987).

Animals. Male Sprague-Dawley rats weighing 250 to 350 g (Harlan Laboratories, San Diego, CA), were housed in a constant temperature and humidity environment, with alternating 12-h light and dark cycles. The rats had free access to water and Purina Rodent Chow ad libitum.

Cell Culture. HeLa cells engineered to express rat Oatp1 under the control of a metallothionein promoter were grown under conditions described previously (Shi et al., 1995). Expression of Oatp1 by stably transfected HeLa/Oatp1 cells was induced by treating cells with 100 μM $ZnSO_4$ for 24 h and an additional 50 μM $ZnSO_4$ for 24 h before harvesting. Cells that were not induced with zinc were treated as control cells.

Taurocholate Uptake and GSH Efflux in Cells. Uptake of [^{3}H]taurocholate was quantified in the absence of albumin as described previously (Satlin et al., 1997). In brief, confluent cells in six-well culture plates (BD Biosciences, San Jose, CA) were washed three times with 1.5 ml of phosphate-buffered saline, pH 7.2. Subsequently, 1.5 ml of 10 μM [^{3}H]taurocholate was added with serum-free buffer A (135 mM NaCl, 1.2 mM $MgCl_2$, 0.81 mM $MgSO_4$, 27.8 mM glucose, 2.5 mM $CaCl_2$, and 25 mM HEPES adjusted to pH 7.2 with NaOH). At various times, cells were harvested by adding 0.4 ml of 5% trichloroacetic acid and radioactivity was determined. Cell protein was determined in replicate by the Bio-Rad protein dye kit (Bio-Rad, Hercules, CA) using bovine serum albumin as a standard. GSH efflux was measured as described previously in control and Oatp1-expressing HeLa cells in buffer A (Lu et al., 1993). Intracellular GSH was prelabeled by incubating cells with trace levels of [^{35}S]cysteine for 12 to 18 h at 37°C. Confluent cells were washed with phosphate-buffered saline, supplemented with 1 mM acivicin, and incubated in 1.5 ml of buffer A at 37°C. Aliquots of the buffer were removed after 15, 30, and 60 min of incubation for determination of radioactivity in a liquid scintillation counter. The efflux of GSH was linear up to 60 min. Cellular levels of GSH were determined by the method of Tietze (1969) or by high-performance liquid chromatography (Fariss and Reed, 1987). The molecular form of radioactivity in the medium and cells was spot checked and confirmed to be [^{35}S]GSH. Effect of DTT (5 mM) or cystine (0.5 mM) was examined by pretreatment of cells for 1 h, followed by their removal during wash. DTT and cystine were added back into the buffer during the efflux study.

Isolation of Hepatic Membrane Vesicles. Hepatic plasma membrane vesicles were isolated as described previously (Meier et al., 1984b). Membrane fractions were stored at −80°C in buffer A (20 mM KCl, 240 mM sucrose, 0.2 mM $CaCl_2$, 0.2 mM $MgCl_2$, 5 mM $KHCO_3$, and 10 mM HEPES/Tris, pH 7.4). The purity and enrichment of various enzymes, including 5′-nucleotidase, in membrane vesicles were determined by assaying their total activity in the presence of 0.1% Triton X-100 (Mittur et al., 2000).

Isolation and Characterization of Side-Sorted Plasma Membrane Vesicles. We used ectopic sialic acid residues on hepatocytes to separate side-sorted fractions by lectin affinity. Isolation of IO membrane was accomplished as described previously (Ishikawa et al., 1990). Mixed plasma membranes (crude membrane fraction) were washed free of sucrose and suspended in 15 ml of 130 mM KCl, 10 mM HEPES/Tris, pH 7.4. The suspension was homogenized in a tight fitting glass Dounce homogenizer (75 strokes) to separate canalicular and sinusoidal membrane domains and incubated with ethanol-free concanavalin A-Sepharose 4B (4 mg/ml lectin, final concentration) for 3 h at 4°C with gentle agitation. The mixture was centrifuged at 200*g* for 10 min. The supernatant contains unbound IO membranes, whereas RO membranes bind to the lectin-Sepharose complex and precipitate out. RO membranes bound to lectin were liberated by incubating the pellet with 200 mM α-methyl mannoside, pH 7.4, under gentle agitation for 1 h at 4°C. The resulting suspension was centrifuged at 200*g* for 10 min to separate free RO membranes. IO and RO membrane fractions were then harvested by

centrifuging the respective supernatants at 105,000*g* (r_{avg}) for 1 h. The pellets were suspended in 6 ml of 250 mM sucrose, 10 mM HEPES/Tris, pH 7.4, and overlaid on a three-step gradient of 38% (w/w), 34% (w/w), and 31% (w/w) sucrose solutions and centrifuged at 195,200*g* (r_{avg}) for 3 h in a SW41 rotor (Beckman Coulter, Fullerton, CA) at 4°C to resolve canalicular plasma membrane vesicles (cLPM) and bLPM fractions. The side-sorted membranes were then sedimented at 105,000*g* (r_{avg}) for 1 h. The resulting fractions were resuspended and vesiculated in buffer A by 20 passes through a 25-gauge needle. Aliquots (200 μl) of the vesicle suspensions were rapidly frozen in liquid nitrogen and stored at −80°C.

Isolation of Membrane Vesicles from Cultured Cells. Plasma membrane vesicles were isolated from 4 to 8 × 10^8 noninduced (control) or Zn^{2+}-induced (Oatp1-expressing) cells as described previously (Leier et al., 1994; Kannan et al., 1999). The membrane fractions were suspended in 0.5 to 1 ml of buffer A by twenty passes through a 25-gauge needle and stored at −80°C. Isolation of side-sorted vesicles was performed as described above.

Assays of Functional Integrity and Sidedness of Membrane Vesicles. The sidedness of hepatic membrane fractions was monitored by the amount of latent 5′-nucleotidase released in the presence of 0.1% (v/v) Triton X-100, and ATP-dependent uptake of taurocholate in cLPM. The orientation of the membrane vesicles from HeLa cells was estimated by the amount of Triton X-100 [0.1% (v/v)] releasable activity of alkaline phosphatase. The expression and activity of Oatp1 was determined by comparing Na^+-independent uptake of taurocholate (10 μM) in membrane vesicles from control and Zn^{2+}-induced HeLa cells. Uptake of alanine, taurocholate, and *l*-glutamate were determined as described previously (Meier et al., 1984a; Mittur et al., 2000). ATP-dependent uptake of [^{3}H]taurocholate (1 μM) was studied at 37°C under a voltage-clamped condition in a buffer that contained a final concentration of 75 mM K^+ and 5 mM ATP. [^{3}H]Alanine and [^{3}H]L-glutamate uptake were studied in the presence or absence of an inwardly directed gradient of Na^+, 100 mM_{out}:0 mM_{in}.

Uptake and Kinetics of Substrates in Membrane Vesicles. The uptake of radiolabeled substrates in vesicles was determined by rapid filtration (Kannan et al., 1999; Mittur et al., 2000). In each preparation and at all substrate concentrations, measurements were made in duplicate and the mean values of the duplicate determinations were used. Initial rates of GSH uptake were estimated at 25°C (37°C for ATP-dependent taurocholate uptake) by addition of 80 μl of incubation buffer to 20 μl of vesicle suspension (20 to 35 μg of protein). Uptake of radiolabeled substrates was stopped at desired time points by addition of 1 ml of ice-cold stop solution. In all studies, membrane vesicles were subjected to one freeze-thaw cycle and used immediately. All membrane fractions were pretreated with 3 mM acivicin for 30 min at 37°C to inhibit γ-GT. Kinetics of GSH transport in vesicles were determined from initial rates (10 s) of zero-trans uptake of [^{35}S]GSH (0.0002, 0.02, 0.2, 0.5, 1, 5, 10, 25, and 50 mM) added to a buffer containing varying amounts of sucrose, 20 mM KCl, 0.2 mM $CaCl_2$, 0.2 mM $MgCl_2$, 5 mM $KHCO_3$, and 10 mM HEPES, adjusted to pH 7.4 with Tris. At concentrations of GSH greater than 1 mM, iso-osmolarity was rigorously maintained by varying the amount of sucrose. The effect of DTT or cystine on GSH uptake was determined by pretreatment of membrane vesicles with DTT (5 mM) or cystine (5 mM) for 1 h at 37°C and adding them in the incubation buffers during uptake. In all studies, uptake of GSH in IO and RO bLPM, control and Oatp1 membrane vesicles, or in the presence or absence of DTT (or cystine) were determined pairwise on the same day. To determine kinetics, transport was terminated at 10 s with an ice-cold stop solution of identical composition as incubation buffer, but without GSH. All determinations of GSH uptake were performed under a voltage clamp by suspending vesicles in 20 mM K^+ and valinomycin (12 μg/mg protein) for 1 h at 37°C. In studies on effects of a H^+ gradient, the pH of membrane vesicles was clamped by equilibration in a 20 mM K^+ buffer, pH 7.4, in the presence of valinomycin and nigericin (each 12 μg/mg of protein) for 1 h at 37°C. Uptake of GSH under an inwardly directed H^+ gradient was measured by initiating uptake with pH 5.6 buffer in membrane vesicles suspended at pH 7.4 and pretreated with nigericin. The effect of membrane potential was evaluated by an inward K^+ diffusion potential induced by valinomycin in the presence of a K^+-gradient (100 mM_{out}:20 mM_{in}). Trans-stimulation of [^{35}S]GSH (1 mM) and [^{3}H]taurocholate (10 μM) uptake was determined by preloading vesicles with 60 μM taurocholate and 1 mM GSH, respectively, by incubation for 1 h at 37°C. Control vesicles were not preloaded but were otherwise handled identically.

Kinetic Analysis and Fitting of Transport Data. Kinetic data were obtained by measuring initial rates of uptake (10 s) and expressed as mean ± S.E.; *n* represents the number of individual membrane vesicles preparations. The kinetics of GSH transport were analyzed by nonlinear, least-squares regression fits to the data using mean values weighted by standard errors, as described previously (Mittur et al., 2000). Significant differences between paired data were determined by two-sided paired Student's *t* test. Significance was set at $p < 0.05$.

Results

Enrichment, Purity, and Functional Integrity of Membrane Vesicles

Hepatic Membrane Vesicles. As in our earlier preparations (Mittur et al., 2000), bLPM fractions were typically enriched 25- to 35-fold in Na^+-K^+-ATPase and de-enriched or not enriched in intracellular organelle markers (not shown). A property of the method used to fractionate bLPM is that cross-contaminating canalicular membranes comprise ≤8% of the total sinusoidal fraction (Meier et al., 1984b). cLPM fractions were pure (free of sinusoidal contamination) and highly enriched with respect to the apical markers Mg^{2+} ATPase and alkaline phosphatase (not shown). The separation and enrichment of marker enzymes in IO and RO bLPM are shown in Table 1. Na^+-K^+-ATPase, a basolateral en-

TABLE 1

Enrichments of marker enzymes in hepatic sinusoidal plasma membrane fractions.

Specific activity is expressed as nanomoles of product formed per milligram of protein per minute. Activity is expressed as change in absorbance per milligram of protein per minute. Relative enrichment is expressed as the mean (± S.E.M.; $n = 4$) ratio of specific activity in membrane fractions to that in homogenate.

Marker Enzymes	Homogenate (specific activity)	Relative Enrichment		
		PM	IO	RO
Na^+, K^+ ATPase	21.1 ± 1.8	41.1 ± 5.6	18.1 ± 2.2	23.3 ± 4.1
Mg^{2+} ATPase	199 ± 44.1	31.9 ± 5.1	2.9 ± 1.0	5.1 ± 1.2
Alkaline phosphatase	12.7 ± 1.7	39.9 ± 8.8	2.0 ± 1.0	3.2 ± 0.7
Glucose 6-phosphatase[a]	66.5, 177.0	N.D.	1.0, 0.6	1.0, 1.0
Acid phosphatase[a]	81.6, 50.2	N.D.	0.6, 0.8	0.5, 1.0
Succinic dehydrogenase[a]	0.13, 0.11	N.D.	0.1, 1.0	0.8, 0.9

N.D. not determined; PM, mixed plasma membrane.

[a] Relative enrichment are values in two preparations ($n = 2$).

zyme, was comparably enriched ~18- and ~23-fold in IO and RO bLPM, respectively (Table 1). Contamination of IO and RO bLPM with canalicular membranes was substantially less than 8%, as estimated by the enrichments of Mg^{2+}-ATPase (3- to 5-fold) and alkaline phosphatase (2- to 3-fold). In addition to bLPM, cLPM were also simultaneously resolved into IO and RO fractions from the same liver. In an isoosmotic reaction medium and in the absence of detergents, the specific activity of alkaline phosphatase (an ectoenzyme) was 10-fold higher in RO cLPM (38-fold enrichment) relative to the inside-out fraction, indicating good separation of the two-sided fractions (not shown).

HeLa Membrane Vesicles. Alkaline phosphatase was enriched 18- to 20-fold in membrane fractions from both control and Oatp1-expressing HeLa cells (Table 2). The membrane fractions were either de-enriched or not enriched in other cell organelle markers (Table 2).

Functional Integrity and Sidedness of Plasma Membrane Vesicles

Hepatic Membrane Vesicles. We used the characteristic overshoot of Na^+-dependent uptake of alanine as a criterion to establish the functional integrity of IO and RO bLPM (Meier et al., 1984a). All IO and RO bLPM used in our studies exhibited at least a 2-fold initial overshoot in alanine uptake over the final equilibrium value (not shown). The uptake of alanine in the absence of Na^+ was minor and did not vary significantly between preparations, indicating consistently minimal 'leakiness' of bLPM. No apparent difference in the passive uptake of alanine was observed in the absence of Na^+ in IO and RO bLPM, indicating that IO and RO bLPM were of comparably high integrity.

The orientation of side-sorted fractions was examined in two independent preparations by the activity of 5′-nucleotidase, an ectoenzyme. Analysis of the total detergent-releasable activity of 5′-nucleotidase indicated that ~85% of the membrane vesicles that did not bind to concanavalin A were oriented inside-out (not shown). A similar analysis of 5′-nucleotidase in the lectin-bound fraction suggested that ~95% were oriented rightside-out (data not shown). As a more pertinent test of the separation of sided membrane fractions, we checked for ATP-dependent uptake of taurocholate in cLPM, which also served to confirm the functional integrity of IO membrane vesicles (Meier et al., 1984a). Reliable assays of asymmetric proteins representing IO bLPM are not known. Therefore, we relied on the homogeneity of simultaneously isolated IO cLPM as an indicator of the goodness and separation of IO bLPM. Because canalicular and sinusoidal membranes were separated after total IO and RO membrane fractions (composed of both canalicular and basolateral domains) were isolated, it is reasonable to expect side-sorted bLPM to reflect the purity and homogeneity of IO and RO cLPM. Hydrolysis of ATP and the resultant ATP-dependent uptake of taurocholate is expected only in IO cLPM. The complete absence of ATP-dependent taurocholate uptake in RO cLPM fractions and at least a 2-fold ATP-dependence in IO cLPM were considered as benchmarks of adequate separation and enrichment in each preparation (Ishikawa et al., 1990). Membrane fractions that did not exhibit greater than 90% homogeneity of the desired orientation were not used. Likewise, a preparation was discarded (including bLPM) if ATP-dependent uptake of taurocholate was observed in rightside-out cLPM. In our preparations, ATP-dependent transport of taurocholate was present exclusively in IO cLPM fractions (not shown), confirming the high degree of separation and functional integrity of membrane vesicles used. The functional integrity of RO cLPM was verified by Na^+-dependent uptake of L-glutamate (not shown) (Ballatori et al., 1986).

HeLa Membrane Vesicles. The orientation of membrane vesicles from control and Oatp1-expressing HeLa cells was estimated by alkaline phosphatase, an ectoenzyme. A comparison of the activities of alkaline phosphatase in the presence and absence of Triton X-100 in two membrane preparations indicated that ~70% of control and Oatp1-enriched vesicles were oriented rightside-out (not shown). The functional expression of Oatp1 in Zn^{2+}-induced HeLa cells was verified in every preparation of membrane vesicles by comparing the time course of taurocholate uptake in membrane vesicles from Oatp1-expressing HeLa cells to those from non-induced, control HeLa cells. As shown in Fig. 1, uptake of taurocholate (20 μM) was 2- to 3-fold higher in membrane vesicles isolated from cells that were induced with Zn^{2+}. A similar result was obtained for uptake of taurocholate at 1 μM (not shown). The substantially higher rate of taurocholate uptake in membrane vesicles from HeLa/Oatp1 cells not only confirms the expression of Oatp1 but also corroborates the functional integrity of membrane vesicles.

GSH Uptake in Sidedness-Sorted Hepatic bLPM

We determined GSH uptake at three concentrations (i.e., 200 μM, 1 mM, and 5 mM) to cover a broad range of affinities of putative transporters. The uptake of GSH tended to be higher in IO bLPM at all levels of GSH tested, including the low end at 200 μM. At 1 mM and 5 mM, the rates of uptake were significantly higher in IO bLPM (Fig. 2 and Table 3). For example, the initial (10 s) rate of GSH uptake at 5 mM in IO and RO bLPM was 3.28 ± 0.56 nmol/mg of protein/10 s

TABLE 2

Enrichments of marker enzymes in HeLa plasma membrane fractions.

Specific activity is expressed as nanomoles of product formed per milligram of protein per minute. Activity of succinic dehydrogenase is expressed as change in absorbance per milligram of protein per minute. Relative enrichment is expressed as the mean (± S.E.M.; n = 5) ratio of specific activity in membrane fractions to that in homogenate.

Marker Enzymes	Control		Oatp1	
	Homogenate (Specific Activity)	PM RE	Homogenate (Specific Activity)	PM RE
Alkaline phosphatase	198 ± 88	18.1 ± 6.5	16.2 ± 4.9	19.8 ± 4.5
Glucose 6-phosphatasase[a]	256 ± 61	0.9 ± 0.3	202 ± 93	1.2 ± 0.5
Acid phosphatase[a]	144 ± 48	1.4 ± 0.5	91 ± 38	1.3 ± 0.4
Succinic dehydrogenase[a]	0.331 ± 0.08	1.4 ± 0.5	0.251 ± 0.11	1.1 ± 0.3

N.D., not determined; PM, mixed plasma membrane; RE, relative enrichment.
[a] n = 4.

and 1.65 ± 0.55 nmol/mg of protein/10 s, respectively, which are significantly different (mean ± S.E.M.; $p < 0.005$). Thus, the rates of GSH transport across the two sides of the sinusoidal membrane were clearly different. In our preparations, Na^+-dependent alanine uptake was somewhat higher in RO bLPM compared with IO bLPM (not shown). However, it is unlikely that such nonspecific factors as dissimilar passive permeability account for the disparate rates of GSH uptake in IO and RO bLPM. First, a higher passive permeability of RO bLPM would dissipate a Na^+ gradient faster, resulting in less transient accumulation of alanine. To the contrary, the overshoot in alanine uptake was greater in RO bLPM, as opposed to GSH uptake, which was higher in IO bLPM. Second, in simultaneously isolated IO and RO cLPM from the same livers, the rate of GSH transport was higher in RO vesicles (not shown). Furthermore, there was no difference in the passive uptake of alanine in IO and RO bLPM, suggesting that IO and RO bLPM were of high integrity. Therefore, our data strongly indicate that rates of efflux and uptake of GSH across sinusoidal plasma membrane are distinct and represent an asymmetric process.

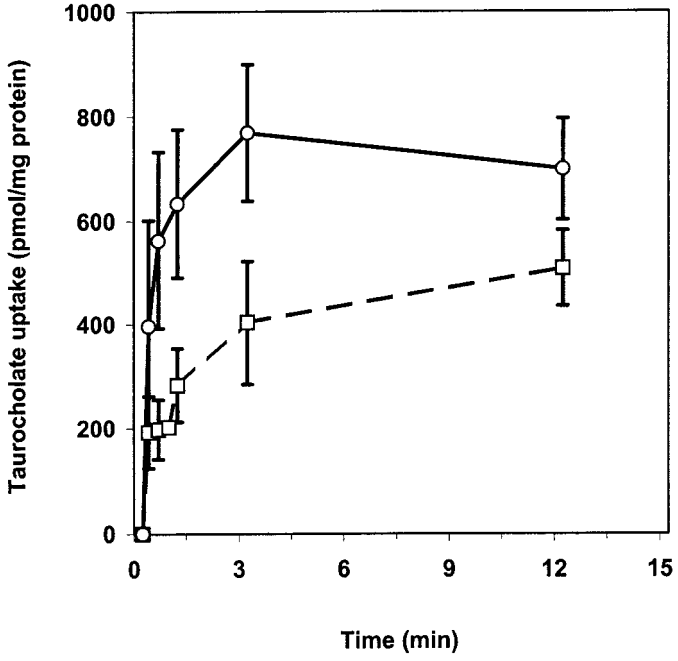

Fig. 1. Time course of sodium-independent uptake of taurocholate. Transport of taurocholate in membrane vesicles from uninduced (□) and zinc-induced (○) HeLa cells was determined at 20 μM (mean ± S.E.M.; $n = 5$).

Effect of DTT on GSH Uptake in Sidedness-Sorted bLPM

The uptake of GSH at 1 mM and 5 mM GSH was determined over a course of 12 min in IO and RO bLPM pretreated with DTT (5 mM) for 1 h. In IO bLPM, DTT selectively and significantly increased uptake at both concentrations by 60 to 90% ($p < 0.05$; Table 3). At 1 mM and 5 mM GSH, rate of uptake in untreated IO bLPM was 2.26 ± 0.11 and 3.28 ± 0.55 nmol/mg of protein/10 s, respectively (mean ± S.E.M.). After pretreatment of IO bLPM with DTT, 1 mM and 5 mM GSH were transported at significantly higher rates of 3.74 ± 0.16 and 5.38 ± 0.50 nmol/mg of protein/10 s, respectively (mean ± S.E.M.; $p < 0.05$). Conversely, pretreatment with DTT tended to inhibit GSH uptake in RO bLPM, although the decrease was not statistically significant (Table 3). To examine whether DTT exerts nonspecific effects on transport in membrane vesicles, we examined its influence on sodium-dependent uptake of alanine and taurocholate in two IO and

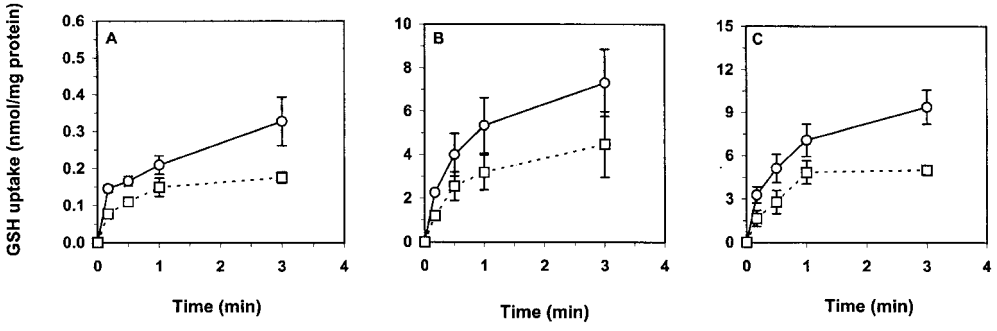

Fig. 2. Time course of GSH uptake in side-sorted sinusoidal membrane vesicles. Uptake of GSH at 200 μM (A), 1 mM (B), and 5 mM (C) under voltage-clamped condition was determined in the absence of DTT in inside-out (○) and rightside-out (□) bLPM as described under *Materials and Methods*. Each point represents the mean ± S.E.M. of three to five independent preparations.

TABLE 3

Effect of DTT on GSH uptake in side-sorted sinusoidal membrane vesicles.

Transport of GSH in untreated and DTT-pretreated inside-out (IO) and rightside-out (RO) sinusoidal membrane vesicles (bLPM) was determined at various levels of GSH under a voltage-clamped condition as described under *Materials and Methods*. Equilibrium values of GSH uptake (12 min) in IO and RO bLPM were not significantly different. Each value represents the mean ± S.E. of at least three independent preparations ($n = 3$–5).

GSH	DTT	GSH Uptake			
		IO bLPM		RO bLPM	
		10 s	30 s	10 s	30 s
		nmol/mg of protein			
200 μM	−	0.146 ± 0.01	0.166 ± 0.01	0.077 ± 0.006*	0.110 ± 0.01*
1 mM	−	2.26 ± 0.11	3.99 ± 0.97	1.19 ± 0.11*	2.55 ± 0.65*
	+	3.74 ± 0.16#	6.25 ± 1.39#	0.56 ± 0.37	1.16 ± 0.52*
5 mM	−	3.28 ± 0.56	5.12 ± 0.99	1.65 ± 0.55**	2.78 ± 0.80*
	+	5.38 ± 0.50#	9.37 ± 2.19#	1.43 ± 0.34**	1.95 ± 0.32*

Significantly different from the respective value in the absence of DTT ($p < 0.05$) using two-sided paired Student's t test.
* Significantly different from the respective value in IO bLPM ($p < 0.05$) using two-sided paired Student's t test.
** Significantly different from the respective value in IO bLPM ($p < 0.005$) using two-sided paired Student's t test.

RO bLPM preparations. Distinct transporters mediate the sodium-dependent uptake of alanine and taurocholate across the basolateral membrane of hepatocytes. The transport of alanine and taurocholate was not altered in IO and RO bLPM that were by pretreated with DTT (not shown). These observations reveal that DTT exerts its asymmetric effects on sinusoidal efflux and uptake of GSH at the level of plasma membrane.

Kinetics of Sinusoidal GSH Transport in Side-Sorted bLPM

We have shown previously that GSH uptake in bLPM of mixed orientation is mediated by two components, a high-affinity component with a low capacity and a low-affinity unit with a high capacity for GSH transport (Ookhtens and Kaplowitz, 1998). At GSH levels below 200 μM, the high-affinity unit was found to mediate greater than 99% of total transport but to facilitate only ~5% of total transport at GSH levels above 25 mM. We examined hypothetical differences in the kinetics of GSH efflux and uptake by characterizing kinetics of uptake in IO and RO bLPM, respectively. Our preliminary attempts to fit the kinetic data for GSH transport in IO and RO bLPM indicated the necessity for inclusion of both high-affinity Michaelis-Menten and low-affinity sigmoid (Hill) components, analogous to and consistent with our mixed orientation bLPM (Mittur et al., 2000). Thereafter, we concentrated on extracting the kinetic parameters with as much precision as possible from our data to resolve whether the changes observed were caused by differences of K_m or V_{max}. Attempts to determine whether the data could be fitted by ascribing changes strictly to K_m values but not V_{max} values ruled out such a possibility. Conversely, allowing adjustment of all parameters independently indicated that the differences in the kinetics of GSH transport in IO versus RO bLPM were essentially all caused by differences in V_{max} and not K_m of the major, quantitatively significant low-affinity component. Therefore, the two data sets were fitted simultaneously, submitting uniform K_m values for the low-affinity component. The resulting fits are shown in Fig. 3 and Table 4 shows the estimated values of the parameters obtained from the fits. As can be seen, although good fits were produced in all ranges of GSH concentrations, only the parameters of the low-affinity components could be resolved with precision. As shown in Fig. 3 and Table 4, GSH uptake in IO and RO bLPM was governed by two kinetically distinct components, including a high-affinity Michaelis-Menten component and a low-affinity sigmoid component. The contribution of the sigmoid transporter to total transport was negligible at GSH levels below 2 to 3 mM (Fig. 3). The V_{max} of the sigmoid component in IO bLPM was ~2-fold higher compared with RO bLPM, which manifests in significantly higher rate of GSH transport in IO bLPM (Table 4). Our modeling indicates that the high-affinity Michaelis-Menten component mediates $\leq$ 5% of total uptake at GSH levels above 2 mM. However, parameters of this relatively minor high-affinity component could not be resolved with adequate precision to ascertain whether changes in that component were caused by changes in K_m, V_{max}, or both.

Oatp1-Dependent Efflux of GSH

We examined the uptake of taurocholate as confirmation for expression of Oatp1 in our cells after Zn^{2+}-induction. Uptake of 10 μM taurocholate by cells that were induced to express Oatp1 was substantially higher than uninduced control cells (not shown), as reported by others (Satlin et al., 1997). We examined basal efflux of GSH and its response to DTT and cystine in control and Oatp1-expressing cells. Figure 4 shows GSH efflux and the effect of these chemicals in control and Oatp1-expressing HeLa cells. Efflux of GSH from Oatp1-expressing HeLa cells was significantly higher compared with control cells (Fig. 4). DTT significantly stimulated efflux of GSH from control cells by 2-fold (Fig. 4), confirming an earlier study (Lu et al., 1993). However, efflux stimulated by DTT was not significant in Zn^{2+}-induced cells and may be attributed to the endogenous carrier in HeLa cells (Fig. 4). On the other hand, efflux of GSH from Oatp1-expressing cells was inhibited by cystine to a significantly greater extent compared with control noninduced cells (Fig. 4). These results suggest that DTT and cystine exert their effects on GSH efflux by influencing different carriers. Our observations on the effect of cystine on GSH efflux from HeLa cells are not unequivocal because HeLa cells require cystine in the medium to support synthesis of GSH (Lu et al., 1993). To better characterize Oatp1-mediated GSH transport, we conducted further studies in isolated plasma membrane vesicles from control and Oatp1-expressing HeLa cells.

GSH Uptake in Membrane Vesicles from HeLa Cells

[^{35}S]GSH uptake was determined at three concentrations (100 μM, 1 mM, and 10 mM) in membrane vesicles from control and Oatp1-HeLa cells in the absence of taurocholate. As with most cells, HeLa cells also exhibit endogenous GSH transport at all levels of GSH tested. The initial rate (10 s) was significantly higher at 1 mM and 10 mM in Oatp1-

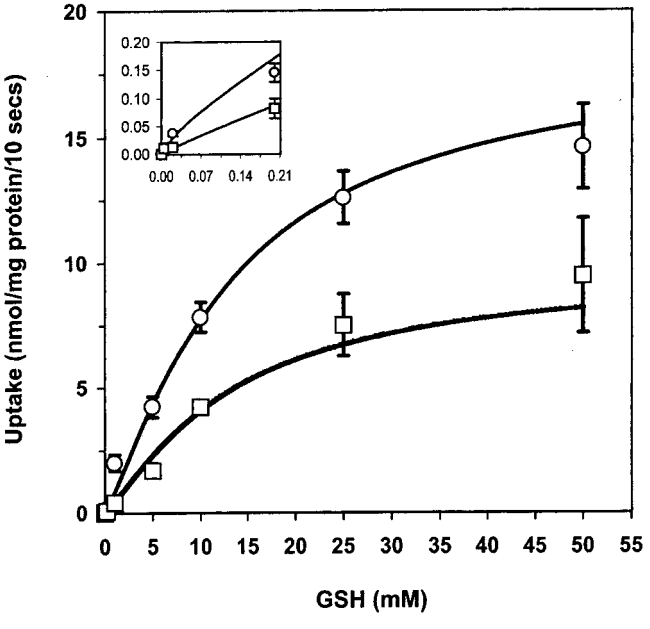

Fig. 3. Kinetics of GSH transport in inside-out and rightside-out sinusoidal membrane vesicles. Initial rates of GSH uptake (10 s) were determined in inside-out (○) and rightside-out (□) vesicles under voltage-clamped conditions from the uptake of [^{35}S]GSH in the presence of GSH concentrations ranging from 0.0002 μM to 50 mM. The best overall fits to total uptake, shown as continuous curves, were obtained by the sum of a Michaelis-Menten (MM) and a sigmoid Hill component as described under *Materials and Methods*. Insets show a magnified scale of the high-affinity region. Each point represents the mean ± S.E.M. of three to four independent preparations.

enriched membrane vesicles ($p < 0.05$, Table 5). However, we did not observe a statistically significant difference between initial rate of GSH uptake at 100 μM in Oatp1 and control membrane vesicles (Table 5). These are the first observations to indicate that GSH is transported by Oatp1 in membrane vesicles and that GSH is a substrate for Oatp1 in the absence of bile salts such as taurocholate.

Influence of DTT and Cystine on GSH Uptake in Membrane Vesicles from HeLa Cells

To examine whether thiols and disulfides influence Oatp1-mediated GSH transport, we determined the time course of uptake in control and Oatp1-enriched vesicles that were pretreated with DTT. DTT (3 mM) inhibited 40 to 60% of uptake in control and 15 to 30% of uptake in Oatp1-enriched vesicles at all levels of GSH tested. GSH uptake at 100 μM in control and Oatp1-enriched membrane vesicles was inhibited by DTT, although the decrease was not significant (Table 5). Pretreatment of control vesicles with DTT resulted in a significant decrease of uptake above 1 mM GSH ($p < 0.05$, Table 5). In contrast, the apparent decrease in uptake of GSH at 1 mM and 10 mM in DTT-treated Oatp1-enriched vesicles was not significant (Table 5). The magnitude of Oatp1-mediated increase in GSH uptake at all concentrations was similar in the presence or absence of DTT, suggesting that DTT inhibited only endogenous GSH transport in HeLa cells and not Oatp1-mediated uptake. GSH uptake was not altered when membrane vesicles (control or Oatp1) were exposed to DTT in the transport buffer but not pretreated (not shown). To rule out nonspecific effects of DTT on substrate transport, we tested the uptake of Na^+-independent taurocholate and Na^+-dependent glutamate uptake in control and Oatp1-enriched vesicles. In two preparations, uptake of neither substrate was altered by DTT in control or Oatp1-enriched vesicles (not shown), further suggesting that DTT exerts a specific effect on endogenous GSH transport in HeLa cells, and not on Oatp1. Pretreatment of control and Oatp1-expressing membrane vesicles with cystine (5 mM) inhibited GSH uptake only in Oatp1-enriched vesicles (36 and 42% inhibition at 5 mM GSH, $n = 2$), consistent with our observations in intact cells (Fig. 4).

To assess the asymmetry of DTT effect on GSH transport in HeLa membrane vesicles, we separated IO and RO membrane fractions from HeLa cells. In two individual preparations, control and Oatp1-enriched IO membrane vesicle fractions were 80 and 65% oriented inside-out, respectively, whereas 85 and 80% of control and Oatp1-enriched membrane vesicle fractions that bound to the lectin were right-side-out. In side-sorted vesicles from uninduced control cells, DTT inhibited the uptake of GSH (1 mM and 5 mM) in rightside-out and tended to enhance uptake in inside-out vesicles (Table 6). The latter was more apparent at 5 mM, consistent with the low affinity of this system (see below). The stimulatory effect of DTT on GSH uptake in IO vesicles was greater in the preparation with 80% IO than the one with 65% IO (Table 6). DTT had a similar effect of comparable magnitude in side-sorted vesicles from Oatp1-enriched vesicles (Table 6).

Effect of Membrane Potential and H^+ Gradient on GSH Uptake in Membrane Vesicles from HeLa cells.

An earlier study has suggested that Oatp1-mediated taurocholate transport can be modulated by an inwardly-directed H^+ gradient, or by exchange with HCO_3^- ions (Satlin et al., 1997). To identify the driving forces of Oatp1-mediated uptake of GSH, we examined the effect of membrane potential and H^+-gradient on Oatp1-mediated GSH uptake in isolated plasma membrane vesicles. An inside-positive K^+ diffusion potential [$K^+_{out:in}$ (mM) = 100:20] significantly increased the rate of GSH uptake at 5 mM in control vesicles (2.34 ± 0.08 to 3.24 ± 0.28 nmol/mg of protein/10 s; mean ± S.E.; $p < 0.05$). A similar effect of inside-positive potential was observed in control vesicles at 10 mM GSH. The uptake of GSH at 5 or 10 mM in Oatp1-enriched vesicles was not significantly further stimulated by the inside-positive potential (not shown). An inwardly directed H^+ gradient (pH_{out}: pH_{in} = 5.6:7.5) had no effect on GSH uptake at 100 μM GSH in control or Oatp1-enriched vesicles, relative to the pH clamped condition (Fig. 5). On the other hand, in the presence of an inwardly-directed H^+ gradient, uptake of 5 and 10 mM GSH was significantly stimulated by up to 100% in Oatp1-containing membrane vesicles exclusively ($p < 0.05$; Fig. 5). The time course of GSH uptake in the presence of the nigericin-induced pH gradient exhibited an overshoot (Fig. 5, d and e). These results suggest that GSH uptake can be driven by a H^+ gradient probably by the exchange of ions such as OH^- (or HCO_3^-) through Oatp1.

An earlier study based on expression of Oatp1 in *X. laevis* oocytes suggested that intracellular GSH serves as a driving force for uptake of organic anions by Oatp1 (Li et al., 1998).

TABLE 4

Comparison of kinetic parameters of GSH uptake in HeLa and sinusoidal membrane vesicles.

Initial rates (10 s) were determined from uptake of [^{35}S]GSH at various concentrations ranging from 0.0002 μM to 50 mM in membrane vesicles under voltage-clamped conditions. Kinetic parameters of GSH uptake in untreated and DTT-pretreated membrane vesicles were estimated by curve fitting using a single Michaelis-Menten component or a combination of a Michaelis-Menten and a sigmoid Hill component as described under *Materials and Methods*. Values in control and Oatp1-expressing HeLa membrane vesicles represent mean ± S.E. (n = 3 to 5); values in IO and RO bLPM represent mean ± S.E. (n = 4 to 5).

Type	DTT	High Affinity		Low Affinity	
		K_m	V_{max}	K_m	V_{max}
		mM	*nmol/mg protein/10 s*	*mM*	*nmol/mg protein/10 s*
bLPM IO	−	0.058 ± 0.064	0.089 ± 0.099	13.2 ± 3.8*	18.4 ± 3.0
bLPM RO	−	0.129 ± 0.231	0.054 ± 0.101	13.2 ± 3.8*	9.69 ± 1.9
HeLa Control	−	N.D.	N.D.	15.3 ± 3.6	23.8 ± 4.2
	+	N.D.	N.D.	13.0 ± 2.4	13.1 ± 2.7
HeLa Oatp1	−	N.D.	N.D.	19.8 ± 2.7	42.1 ± 4.2
	+	N.D.	N.D.	17.8 ± 4.7	32.7 ± 4.9
	adj.	N.D.	N.D.	15.9 ± 1.9	32.2 ± 2.7

N.D., none detected; adj., the fraction of GSH uptake inhibited by DTT in control vesicles was subtracted from uptake in untreated Oatp1 vesicles.
*, sigmoid component with Hill coefficient > 1.2.

To deduce the *trans* effects of taurocholate and GSH on each other, we evaluated *trans*-stimulation of uptake. In two preparations, uptake of taurocholate (60 μM) in Oatp1-enriched vesicles was stimulated by 1 mM *trans*-GSH (439 and 542 pmol/mg of protein/10 s versus 783 and 776 pmol/mg of protein/10 s). By comparison, taurocholate uptake in vesicles from control HeLa cells was unchanged by *trans*-GSH (90 and 95 pmol/mg of protein/10 s versus 98 and 109 pmol/mg of protein/10 s) which is consistent with negligible transport of taurocholate in control HeLa cells (Shi et al., 1995; Satlin et al., 1997). Uptake of GSH (1 mM) was not enhanced by *trans*-taurocholate (60 μM) in Oatp1-enriched vesicles, perhaps because of poor sensitivity and high endogenous GSH transport (not shown).

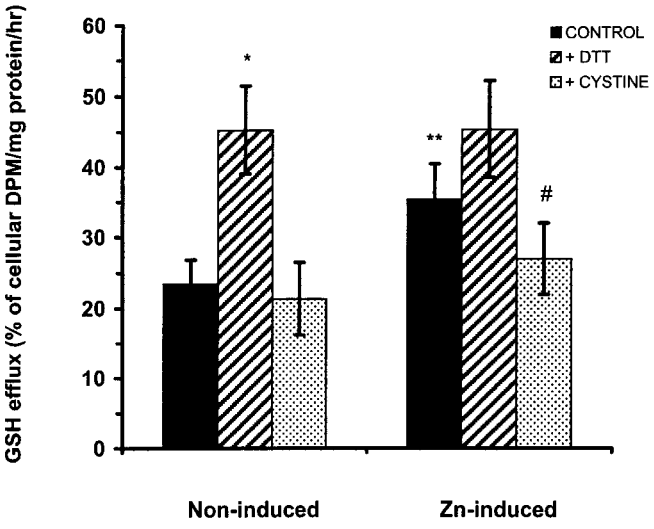

Fig. 4. GSH efflux and effect of DTT and cystine in zinc-induced and noninduced Oatp1-transfected HeLa cells. [^{35}S]GSH efflux was measured as described under *Materials and Methods*. Effect of DTT (5 mM) and cystine (0.5 mM) as examined by pretreating cells with DTT or cystine for 1 h and adding them in the efflux medium. Results are expressed as mean ± S.E.M. (n = 3). GSH efflux is expressed as a percentage of total cellular radioactivity that appears in the medium at 1 h. The molecular form of the label in the medium was confirmed by HPLC. *, $p < 0.05$ versus noninduced control cells; ** $p < 0.05$ versus noninduced control cells; and #, $p < 0.05$ versus zinc-induced control cells, as determined by two-sided paired Student's t test.

Kinetics of Oatp1-Mediated GSH Transport and Effect of Thiol

To further characterize Oatp1-mediated GSH uptake, we determined kinetics of uptake in membrane vesicles from Oatp1-expressing HeLa cells and compared it to those from control HeLa cells. The results of kinetic analysis by nonlinear curve fitting to GSH uptake in the two populations are shown in Fig. 6. In vesicles from control HeLa cells, transport of GSH was mediated by a single Michaelis-Menten component with a low affinity (K_m = 15.3 ± 3.6 mM; Fig. 6). In vesicles pretreated with DTT, the V_{max} of the Michaelis-Menten component decreased by 50%, whereas affinity remained unchanged at 13.0 ± 2.4 mM (Fig. 6; Table 4). Compared with control vesicles, the maximal capacity of GSH uptake in Oatp1-enriched vesicles was higher, whereas the K_m value remained unchanged (~ 17 mM). DTT tended to decrease total uptake of GSH in Oatp1-enriched vesicles as well. However, as shown above, the portion of GSH uptake attributable to Oatp1 was not significantly affected by DTT at various levels of GSH examined, indicating that DTT

TABLE 5

Effect of DTT pretreatment on GSH uptake in control and Oatp1-enriched membrane vesicles from HeLa cells.

Transport of GSH in untreated and 3 mM DTT-pretreated membrane vesicles was determined under a voltage-clamped condition as described under *Materials and Methods*. Equilibrium values of GSH uptake (12 min) in control and Oatp1-enriched membrane vesicles were not significantly different. Each value represents the mean ± S.E.M. in three (100 μM) or five (1 mM and 10 mM) independent preparations (except in DTT pretreated, where n = 3).

GSH	Rate of Uptake			
	Control		Oatp1-Enriched	
	− DTT	+ DTT	− DTT	+ DTT
	nmol/mg of protein/10 s			
100 μM	0.368 ± 0.11	0.185 ± 0.07	0.461 ± 0.16	0.252 ± 0.11
1 mM	0.680 ± 0.10	0.329 ± 0.07#	2.01 ± 0.40*	1.31 ± 0.20*
10 mM	7.89 ± 0.92	4.02 ± 0.45#	14.7 ± 2.37*	13.0 ± 0.98*

Significantly different from the respective values in the absence of DTT ($p < 0.05$) using two-sided paired Student's t test; *, significantly higher than the respective values in controls ($p < 0.05$) using two-sided paired Student's t test.

TABLE 6

Effect of DTT on GSH uptake in side-sorted membrane vesicles from control and Oatp1-expressing HeLa cells.

Transport of GSH in untreated and DTT-pretreated inside-out (IO) and rightside-out (RO) membrane vesicles (LPM) from control and Oatp1-expressing HeLa cells was determined at various levels of GSH under a voltage-clamped condition as described under *Materials and Methods*. IO and RO membranes were prepared from each of four cell preparations. The average values of duplicate measurements in two individual preparations from control and Oatp1 expressing cells are shown. IO preparations 1 and 3 were 80 and 85% inside-out whereas preparations 2 and 4 were 65% inside-out. RO preparations were all 80 to 85% rightside-out.

GSH	DTT (5 mM)	GSH Uptake							
		IO LPM				RO LPM			
		Control Prep		Oatp1 Prep		Control Prep		Oatp1 Prep	
		1	2	3	4	1	2	3	4
		nmol/mg of protein/10 s							
1 mM	−	2.14	1.86	3.28	3.16	2.37	1.77	2.98	2.56
	+	2.62	1.72	3.48	2.31	1.34	0.76	2.15	1.49
5 mM	−	7.93	2.65	11.2	5.15	6.94	4.90	10.1	11.3
	+	13.6	2.82	18.8	7.21	0.81	1.27	3.06	4.84

modulates the endogenous transporter. Analyzing the effect of DTT on kinetics of GSH uptake in Oatp1-enriched vesicles indicated that although the affinity remained unchanged, V_{max} decreased by ~10 nmol/mg of protein/10 s in the presence of DTT. This decrease was identical in magnitude to the reduction in V_{max} of the endogenous transporter by DTT (Table 4; Fig. 6). As an alternative exercise to clarify whether kinetics of GSH uptake by Oatp1 is changed by DTT, we subtracted the fraction of total uptake inhibited by DTT in control vesicles (see Fig. 6) from uptake in Oatp1-enriched vesicles measured in the absence of DTT. The resulting adjusted values for uptake in Oatp1 vesicles and the resultant kinetic fit were virtually identical to that seen in DTT-pretreated Oatp1 vesicles (Fig. 6), indicating that the effect of DTT in Oatp1 vesicles could be accounted for solely by the endogenous GSH transporter.

Discussion

DTT, an uncharged dithiol, enhances efflux of GSH but decreases its uptake in hepatocytes (Lu et al., 1993, 1994). The opposing effects of thiols and disulfides on sinusoidal GSH transport suggest asymmetry in transport pathway(s) that may be modulated by the redox status of hepatic cytosol and blood plasma. Redox changes in the intra- and extrahepatic environment during sustained oxidative challenge and diseases may alter GSH homeostasis (Sen and Packer, 1996; Samiec et al., 1998). The site and mechanism of action of thiols and disulfides on sinusoidal GSH transport are not known. Thiols and disulfides may influence cellular secretion of GSH by directly interacting with transporter(s) or indirectly by acting at other intracellular sites and organelles. Thiols and disulfides are known to asymmetrically regulate transporters, such as sarcoplasmic reticulum Ca^{2+}-ATPase and the facilitative glucose transporter, GLUT1 (Zaidi et al., 1989; Hebert and Caruthers, 1992). Models that have been used to study the effects of thiols and disulfides on GSH transport, including hepatocytes, cultured cell lines and perfused livers, cannot unequivocally differentiate mechanisms of action from multiple possibilities. Attempts to study the effect of thiols on GSH uptake in hepatic plasma membrane vesicles has been hampered due to their mixed orientation (M. Ookhtens and A. Mittur, unpublished observations).

It has been speculated that the contradictory effects of DTT on GSH transport may be caused by kinetic asymmetry of one or more transporters (Lu et al., 1993, 1994). In bLPM of mixed orientation, only a fraction of net uptake is representative of efflux, because ~40% of the vesicles are inside-out (Meier et al., 1984b). DTT does not influence GSH uptake in bLPM of mixed orientation (M. Ookhtens and A. Mittur, personal communication), but this could be because the opposing effects of GSH uptake on efflux and uptake mask its modulation by DTT. We therefore characterized the regulation of sinusoidal GSH transport by thiols in sidedness-sorted IO and RO bLPM. At physiological levels, DTT stimulated GSH uptake by up to 100% in IO bLPM, consistent with its effect on GSH efflux from cells. In RO bLPM, DTT tended to decrease GSH uptake at all levels tested, although not significantly. The magnitude of DTT-mediated stimulation in IO bLPM was less than that observed in perfused liver and certain cells, suggesting that other factors may be essential for optimal function of the primary GSH transporter. The opposing effects of DTT on GSH uptake in IO and RO bLPM are indicative of the inherent asymmetry in sinusoidal GSH transport.

The specific rate and kinetics of GSH uptake in IO and RO bLPM were different. GSH uptake was consistently higher in IO bLPM than RO bLPM, indicating that efflux of GSH from hepatocytes may occur at a higher rate than uptake. A sigmoid, low-affinity transport component was present in both IO and RO bLPM with similar affinity and Hill coefficient. The capacity for GSH efflux from the sinusoidal domain may be higher than that for uptake as observed by the higher V_{max} for GSH uptake in IO bLPM. A high-affinity Michaelis-Menten component was also present in IO and RO bLPM and mediates less than 5% of total uptake above 2 mM GSH. Thus, the higher rate of GSH uptake observed in IO bLPM is attributable to the higher capacity of the sigmoid component. The different transport rates and the thiol-sensitivity of GSH transport in IO and RO bLPM reveal that efflux and uptake

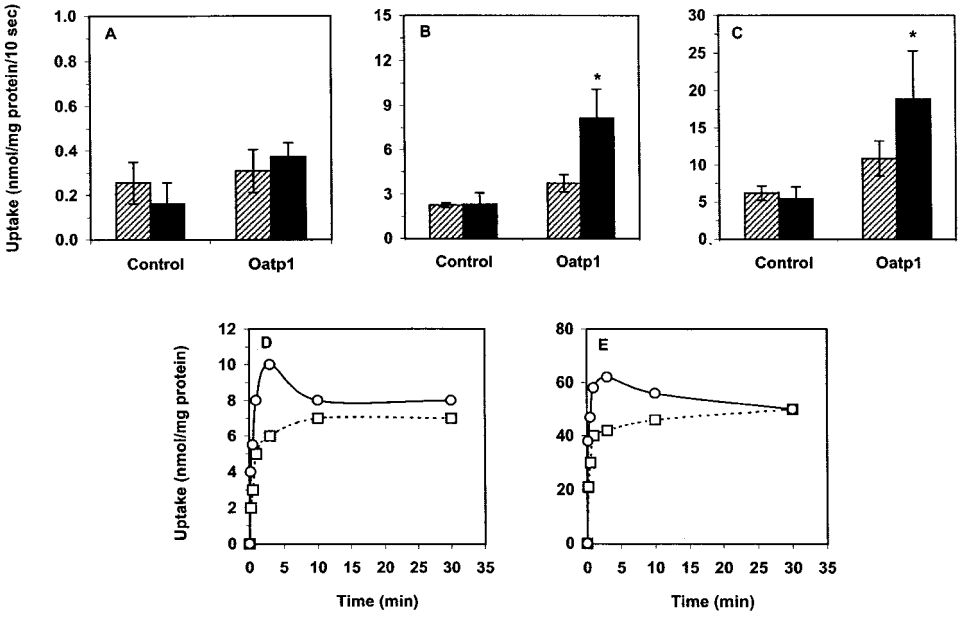

Fig. 5. Effect of H^+ gradient on GSH uptake. Uptake of GSH at 100 μM (A), 5 mM (B), and 10 mM (C) was determined under pH clamped (▨, pH_{out}:pH_{in} = 7.5:7.5) or inwardly-directed H^+ gradient (■; pH_{out}:pH_{in} = 5.6:7.5) in control and Oatp1-enriched membrane vesicles as described under *Materials and Methods*. Each point in A, B, and C represents the mean ± S.E.M. of at least three independent preparations (n = 3–4). *, $p < 0.05$, significantly higher than uptake under pH clamped condition. The time course of GSH uptake at 1 mM (D) and 10 mM (E) was examined in two different preparations under pH clamped (□) or inwardly-directed H^+ gradient (○) in Oatp1-enriched membrane vesicles as described under *Materials and Methods*.

of GSH across the sinusoidal membrane of hepatocytes is asymmetric.

The thiol-sensitive GSH transporter in the basolateral membrane of hepatocytes remains to be identified. Two basolateral organic anion transporters of the OATP (SLC21) transporter family, Oatp1 and Oatp2, have been reported to transport GSH to different extents in *X. laevis* oocytes (Li et al., 1998, 2000). Oatp1 has been proposed to use at least two distinct driving forces: counter exchange of organic anions, such as GSH (Li et al., 1998), and transport driven by the exchange of ions such as OH^- and HCO_3^- (Shi et al., 1995). Our study indicates that an inwardly directed H^+ gradient stimulates GSH uptake in Oatp1-enriched vesicles. The higher rate of GSH and taurocholate uptake in Oatp1-enriched vesicles indicates that a more prevalent ion(s) may serve as an exchange substrate in our assay system. Because GSH uptake in Oatp1-enriched vesicles is stimulated by a H^+ gradient, it is likely that movement of ubiquitous ions (such as OH^- or HCO_3^-) drives a compensatory flux of ions through Oatp1 in exchange with GSH. This is consistent with previous observations of taurocholate uptake by Oatp1 (Shi et al., 1995). The significantly higher uptake of GSH observed in Oatp1 vesicles in the absence of *trans*-taurocholate suggests that taurocholate is not necessary for the exchange of GSH by Oatp1. Likewise, GSH does not seem to be an obligate exchange substrate for taurocholate transport by Oatp1. Membrane potential, which strongly influences sinusoidal GSH transport by a high-capacity, low-affinity carrier (Aw et al., 1984; Fernandez-Checa et al., 1993; Lu et al., 1993, 1994) had no effect on GSH uptake by Oatp1. Notably, transport of GSH by the endogenous carrier in HeLa cells was electrogenic. GSH transport in membrane vesicles from control HeLa cells was mediated by a single transporter (K_m = 15 mM). Expression of Oatp1 resulted in an almost 2-fold increase in maximal capacity of uptake in membrane vesicles, whereas K_m remained unchanged.

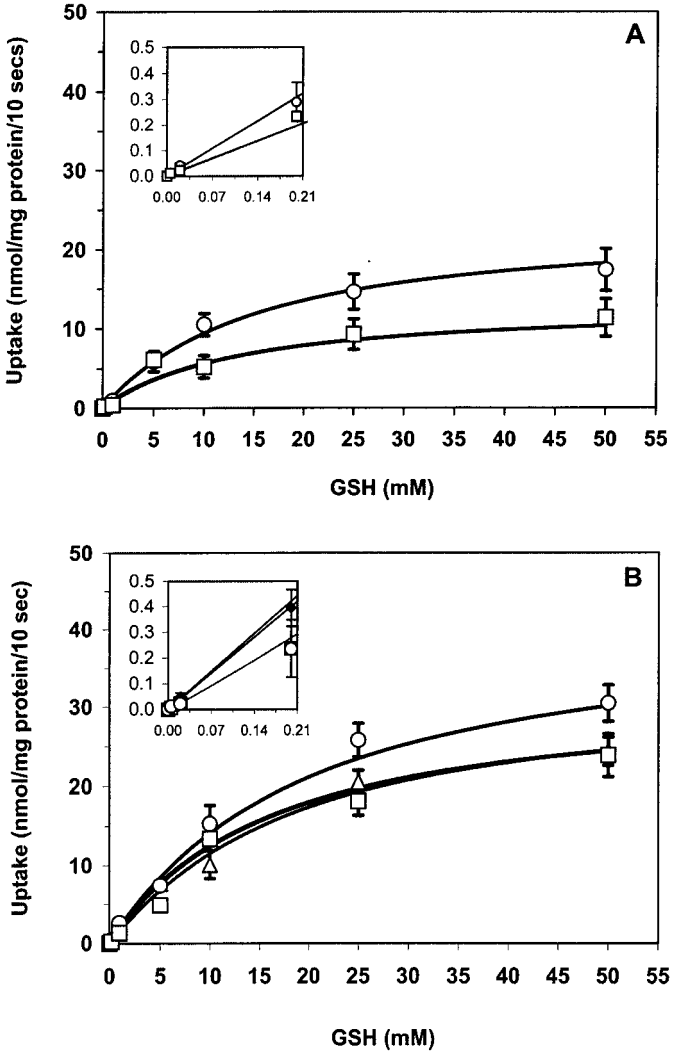

Fig. 6. Kinetics of GSH transport in control and Oatp1-enriched membrane vesicles. Initial rates of transport (10 s) were determined in untreated (○) and DTT-pretreated membrane vesicles (□) from control (A) and Oatp1-expressing HeLa cells (B) under voltage-clamped conditions from the uptake of [^{35}S]GSH at concentrations ranging from 0.0002 μM to 50 mM. The curves represent overall fits to uptake obtained using a single Michaelis-Menten component as described under *Materials and Methods*. Uptake in untreated Oatp1 vesicles in the absence of DTT was also analyzed by subtracting the fraction of GSH uptake in control vesicles that was inhibited by DTT (△, B). Insets show uptake rates at lower concentrations of GSH. Data represent mean ± S.E.M., n = 3–5.

The uptake of taurocholate by Oatp1 has been reported to be insensitive to DTT but the effect of DTT on Oatp1-mediated GSH transport was not investigated (Li et al., 1998). In membrane vesicles from HeLa control cells, GSH uptake was significantly decreased in the presence of DTT. Conversely, the DTT-mediated decrease in GSH transport in Oatp1-enriched membrane vesicles was fully attributable to the decrease observed in vesicles from HeLa control cells. In HeLa cells, DTT increased the efflux of GSH with little effect, if any, on the fraction of GSH efflux mediated by Oatp1. Therefore, the interpretation of our data is that DTT does not influence Oatp1 but modulates an endogenous transporter of GSH present in HeLa cells. It is unlikely that endogenous GSH uptake in control HeLa membrane vesicles may have masked any minor effects of DTT on Oatp1. The inhibition of GSH uptake by DTT in vesicles from HeLa cells results in decreased capacity of the endogenous transporter(s) without altering its affinity. Thus, the endogenous transporter for GSH in HeLa cells seems to be functionally similar to the electrogenic, thiol-sensitive sinusoidal GSH carrier. In contrast to thiols, cystine selectively inhibited efflux of GSH by Oatp1 in cells and membrane vesicles. Endogenous efflux of GSH in HeLa cells was not altered by cystine. Therefore, the distinct effects of thiols and disulfides on GSH efflux is caused by their distinct sites of action; i.e., thiols modulate an endogenous GSH carrier whereas disulfides inhibit Oatp1-dependent GSH efflux. Thus, the thiol-sensitive GSH transporter in HeLa cells and bLPM remains to be identified. The apparent contradictory effects of DTT on GSH efflux from HeLa cells (stimulation) and on its uptake in HeLa membrane vesicles (inhibition) may reflect its asymmetric effects on GSH transport as observed in sidedness-sorted IO and RO bLPM. The plasma membrane vesicles from HeLa cells used in this study were a predominant mixture of rightside-out membranes. Initial attempts to determine the effect of thiols on GSH uptake in IO and RO vesicles from HeLa cells indicate that DTT has distinct effects on GSH uptake in IO and RO LPM from HeLa cells. We observed the same phenomenon as in bLPM: DTT inhibited uptake in RO and tended to enhance uptake in IO vesicles, and this effect was independent of the expression of Oatp1.

The expression of Oatp2 in *X. laevis* oocytes resulted in an

increase in GSH efflux over corresponding water-injected oocytes (Li et al., 2000). Intracellular GSH (10–40 mM) enhanced the uptake of taurocholate and digoxin by Oatp2 (Li et al., 2000). This stimulatory effect of intracellular GSH on taurocholate uptake by Oatp2 was not caused by counter exchange, although the low rates of transport could not exclude this with certainty (Li et al., 2000). The contribution of Oatp2 to GSH transport and the effect of DTT and cystine remain to be clarified, but as with Oatp1, Oatp2 is not expected to account for electrogenic transport of GSH.

In addition to Oatp1 and Oatp2, two transporters of the MRP family, namely multidrug resistance protein 1 (Mrp1) and multidrug resistance protein 2 (Mrp2) have been reported to transport GSH in hepatocytes. Whereas Mrp2 is an apical transporter, Mrp1 is present on the lateral surface of hepatocytes but is normally expressed at very low levels in the liver. Transport by Mrp1 and Mrp2 is not electrogenic and the effects of thiols and disulfides on GSH transport by Mrp1and Mrp2 are not known.

This study has identified that efflux of GSH across the hepatic sinusoidal membrane occurs at a rate higher than uptake, which may be attributed to as-yet-unidentified transporter(s). The marked asymmetry in efflux and uptake of GSH and thiol-effects across the sinusoidal membrane may represent a mechanism to dynamically regulate cellular and extracellular levels of GSH. Our studies reveal that GSH is transported by Oatp1 in the absence of taurocholate, is thiol-insensitive but inhibited by disulfide (cystine). Thus, Oatp1 exhibits only some of the functional features of hepatic sinusoidal GSH transport and does not seem to be the sole transporter of GSH.

Acknowledgments

Plasma membrane vesicles were prepared and provided by the Subcellular-Organelle Core and mathematical analyses and fitting of the data were conducted by the Kinetic and Mathematical Modeling Core of USC Research Center for Liver Diseases.

References

Aw TY, Ookhtens M, and Kaplowitz N (1984) Inhibition of glutathione efflux from isolated rat hepatocytes by methionine. *J Biol Chem* **259:**9355–9358.
Aw TY, Ookhtens M, Ren C, and Kaplowitz N (1986) Kinetics of glutathione efflux from isolated rat hepatocytes. *Am J Physiol* **250:**G236–G243.
Ballatori N, Moseley RH, and Boyer J (1986) Sodium gradient-dependent L-glutamate transport is localized to the canalicular domain of liver plasma membranes: studies in rat liver sinusoidal and canalicular membrane vesicles. *J Biol Chem* **261:**6216–6221.
Fariss MW and Reed DJ (1987) High-performance liquid chromatography of thiols and disulfides: dinitrophenol derivatives. *Methods Enzymol* **143:**101–109.
Fernandez-Checa JC, Ookhtens M, and Kaplowitz N (1993) Selective induction by phenobarbital of the electrogenic transport of glutathione and organic anions in rat liver canalicular membrane vesicles. *J Biol Chem* **268:**10836–10841.
Garcia-Ruiz C, Fernandez-Checa JC, Ookhtens M, and Kaplowitz N (1992) Bidirectional mechanism of plasma membrane transport of reduced glutathione in intact rat hepatocytes and membrane vesicles. *J Biol Chem* **267:**22256–22264.
Ghibelli L, Fanelli C, Rotilio G, Lafavia E, Coppola S, Colussi C, Civitareale P, and Ciriolo MR (1998) Rescue of cells from apoptosis by inhibition of active GSH extrusion. *FASEB J* **12:**479–486.
Hebert DN and Caruthers A (1992) Glucose transporter oligomeric structure determines transporter function: reversible redox-dependent interconversions of tetrameric and dimeric GLUT1. *J Biol Chem* **267:**23829–23838.
Inoue M, Kinne R, Tran T, and Arias IM (1984) Glutathione transport across hepatocyte plasma membranes. Analysis using isolated rat-liver sinusoidal membrane vesicles. *Eur J Biochem* **138:**491–495.
Ishikawa T, Muller M, Klunemann C, Schaub T, and Keppler D (1990) ATP-dependent primary active transport of cysteinyl leukotrienes across liver canalicular membrane: role of the ATP-dependent transport system for glutathione S-conjugates. *J Biol Chem* **265:**19279–19286.
Kannan R, Mittur A, Bao Y, Tsuruo T, and Kaplowitz N (1999) GSH transport in immortalized mouse brain endothelial cells: evidence for apical localization of a sodium-dependent GSH transporter. *J Neurochem* **73:**390–399.
Kaplowitz N, Fernandez-Checa J, and Ookhtens M (1990) Hepatic Glutathione Transport, in *Glutathione Centennial: Molecular Perspectives and Clinical Implications* (Taniguchi N, Higashi T, Sakamoto Y, and Meister A eds), pp 395–406, Academic Press, California.
Kaplowitz N, Aw TY, and Ookhtens M (1985) The regulation of hepatic glutathione. *Ann Rev Pharmacol Toxicol* **25:**715–744.
Leier I, Jedlitschky G, Buchholz U, and Keppler D (1994) Characterization of the ATP-dependent leukotriene C4 export carrier in mastocytoma cells. *Eur J Biochem* **220:**599–606.
Li LQ, Lee TK, Meier PJ, and Ballatori N (1998) Identification of glutathione as a driving force and leukotriene C4 as a substrate for oatp1, the hepatic sinusoidal organic solute transporter. *J Biol Chem* **273:**16184–16191.
Li L, Meier PJ, and Ballatori N (2000) Oatp2 mediates bidirectional organic solute transport: a role for intracellular glutathione. *Mol Pharmacol* **58:**335–340.
Lu SC, Ge J, Huang H, Kuhlenkamp J, and Kaplowitz N (1993) Thiol-disulfide effects on hepatic glutathione—studies in cultured rat hepatocytes and perfused livers. *J Clin Invest* **92:**1188–1197.
Lu SC, Kuhlenkamp J, Ge J, Sun W, and Kaplowitz N (1994) Specificity and directionality of thiol effects on sinusoidal glutathione transport in rat liver. *Mol Pharmacol* **46:**578–585.
Meier PJ, Meier-Abt AS, Barrett C, and Boyer JL (1984a) Mechanism of taurocholate transport in canalicular and basolateral rat liver plasma membrane vesicles: evidence for an electrogenic canalicular organic anion carrier. *J Biol Chem* **259:**10614–10622.
Meier PJ, Sztul ES, Reuben A, and Boyer JL (1984b) Structural and functional polarity of canalicular and basolateral plasma membrane vesicles isolated in high yield from rat liver. *J Cell Biol* **98:**991–1000.
Mittur AV, Kaplowitz N, Kempner ES, and Ookhtens M (2000) Radiation inactivation studies of hepatic sinusoidal reduced glutathione transport system. *Bioch Biophy Acta* **1464:**207–218.
Ookhtens M, Hobdy K, Corvasce MC, Aw TY, and Kaplowitz N (1985) Sinusoidal efflux of glutathione in the perfused rat liver. *J Clin Invest* **75:**258–265.
Ookhtens M and Kaplowitz N (1998) Role of the liver in interorgan homeostasis of glutathione and cyst(e)ine. *Semin Liv Dis* **18:**313–329.
Ookhtens M, Lyon I, Fernandez-Checa JC, and Kaplowitz N (1988) Inhibition of GSH efflux in the perfused rat liver and isolated hepatocytes by organic anions and bilirubin: kinetics, sidedness, and molecular forms. *J Clin Invest* **82:**608–616.
Satlin LM, Amin V, and Wolkoff AW (1997) Organic anion transporting polypeptide mediates organic anion/HCO_3^- exchange. *J Biol Chem* **272:**26340–26345
Samiec PS, Drews-Botsch C, Flagg EW, Kurtz JC, Sternberg P Jr, Reed RL and Jones DP (1998) Glutathione in human plasma: decline associated with aging, age-related macular degeneration, and diabetes. *Free Rad Biol Med* **24:**699–704.
Sen CK and Packer L (1996) Antioxidant and redox regulation of gene transcription. *FASEB J* **10:**709–720.
Shi X, Bai S, Ford AC, Burk RD, Jacquemin E, Hagenbuch B, Meier PJ, and Wolkoff AW (1995) Stable inducible expression of a functional rat liver organic anion transport protein in HeLa cells. *J Biol Chem* **270:**25591–25595.
Tietze F (1969) Enzymic method for quantitative determination of nanogram amounts of total and oxidized glutathione: applications to mammalian blood and other tissues. *Anal Biochem* **27:**502–522.
Zaidi NF, Lagenaur CF, Abramson JJ, Pessah I, and Salama G (1989) Reactive disulfides trigger Ca^{2+} release from sarcoplasmic reticulum via and oxidation reaction. *J Biol Chem* **264:**21725–21736.

Address correspondence to: Neil Kaplowitz, M.D., USC School of Medicine, 2011 Zonal Ave., HMR-101, Los Angeles, CA 90033. E-mail: kaplowit@hsc.usc.edu